photonics

MDPI

Review

High-Power Passive Fiber Components for All-Fiber Lasers and Amplifiers Application—Design and Fabrication

Dorota Stachowiak

Laser Sensing Laboratory, PORT Polish Center for Technology Development, Stablowicka 147, 54-066 Wroclaw, Poland; dorota.stachowiak@port.org.pl

Received: 26 September 2018; Accepted: 15 October 2018; Published: 18 October 2018

Abstract: The most important components for application in high-power all-fiber lasers and amplifiers are, most of all, power combiners, but also mode field adaptors. This paper summarizes recent achievements in the area of development and fabrication of high-power passive fiber components. The principles of operation and basic design and fabrication criteria, which have to be taken into account while designing the aforementioned components, are explained in detail. The most recent impressive achievements are summarized and described.

Keywords: power combiner; mode field adaptor; taper; tapered fused bundle; passive fiber component; all-fiber laser; all-fiber amplifier

1. Introduction

High-power fiber sources operating in the near- and mid-infrared spectral regions are very attractive due to many possible applications, including free-space communications, light detection and ranging (LiDAR) systems, range finding, remote sensing or micromachining [1–3]. In most cases it is very beneficial to have all-fiber construction of lasers and amplifiers, in which all bulk optics components (such as lenses, mirrors, or beam combiners) are replaced with passive fiber-based components. All-fiber construction makes setups significantly less complex, more robust, and immune to external factors, such as vibrations, contamination, or long-term thermal drifts of optomechanical components [4]. In all-fiber configuration it is also easier to maintain high beam quality as the light does not leave the waveguide (i.e., fiber core) during the amplification process. Driven by the needs of existing and possible applications, the operating power of such sources can reach multi-kW power levels. As a result, the design and fabrication of passive fiber components becomes more and more challenging because they have to provide high coupling efficiency at very high power levels.

In order to achieve high output power in a fiber-based system a MOPA (Master Oscillator Power Amplifier) configuration is often utilized. In MOPA, a low-power laser source (Master Oscillator) is used to guarantee high beam quality and the required spectral parameters (e.g., tunability and linewidth). Such a signal is then amplified by a cascade of amplifiers (usually two or three). In such a configuration optical fibers (both passive and active) with different dimensions, mode-field diameters and numerical apertures are typically used. The first amplifier stage frequently utilizes single-mode single-clad (SM-SC) fibers providing output power of up to ~1 W. The signal for amplification and pump light are launched together into the active core (gain medium) using commercially available, off-the-shelf Wavelength Division Multiplexers (WDMs) couplers. The second amplifier stage can be designed for medium-power amplification; a single-mode double-clad (SM-DC) active fiber is often used. In this case, the amplified signal propagates inside the active core, whereas the pump power is launched into the inner cladding with much larger cross-sectional area than the core. This allows

using higher levels of pump power while maintaining reasonably low optical power density per unit area [5]. Thanks to the use of SM-DC active fibers the signal can be amplified up to several watts. The third amplifier stage is used when the output power above dozens watts is needed. This typically requires using large mode area double clad (LMA-DC) fibers which can handle high-power signal and pump light. With increased core diameter (typically up to between 20 and 50 μm) optical power density is reduced which helps to mitigate nonlinear effects such as Stimulated Brillouin Scattering (SBS). However, in order to achieve stable operation of an all-fiber MOPA system at multi-watt levels, it is critical to use special components which enable combining signal and multiple pump sources and connecting different types of fiber with high efficiency and low losses.

The development of DC active fibers was an important step that enabled further evolution and output power scaling of the fiber lasers and amplifiers [6]. As a result, launching the pump power (usually from multiple sources) into the inner cladding with minimal transmission losses and at low-cost became critical part of MOPA systems. Over the years different pumping schemes, including bulk optics, have been developed which can be divided into two categories: side-pumping (through v-groove [7]) and end-pumping methods [8,9]. Pumping through the v-grove is complex. It requires precise grinding-down of the outer clad, cutting the inner cladding to create the v-grove and, in addition, the application of the bulk optics components-based optical setup (e.g., utilizing lenses). This typically results in pump launching efficiency on a level of approximately 70%. An end-pumping scheme is less complex and often provides pump launching efficiency above 90%. However, it also requires using the optical setup (based on bulk optics components). Realization of these schemes is quite challenging, because they require very precise mechanical and optical adjustment, making the laser or amplifier setup very complex and sensitive to external factors (e.g., vibrations, contaminations, and thermal drifts of optomechanical components) [10–13]. In both cases, schemes become even more complex when there is more than one pump source and an additional signal source because the number of bulk optics elements increases.

One can avoid bulk optics components by replacing them with passive fiber components. Then, in a so-called all-fiber configuration, the system does not require periodic adjustments, is less complex, more robust, and immune to external factors. Additionally, because the laser beam is not leaving the fiber core, it is easier to maintain its high quality at the output. The most important passive fiber component in the all-fiber laser and amplifier configuration is the power combiner. Power combiners are used either to launch only pump power into the active fiber inner cladding, or to launch both the pump and the signal simultaneously into the inner cladding and core of the active DC fiber, respectively [4,13–17]. Whereas, in the case of connecting two fibers of different core size and mode field diameter, one can use an MFA—mode field adaptor.

In this paper a review of passive fiber components i.e., power combiners and mode field adaptors. Section 2 concentrates on the general description of principle of operation and their construction. Section 3 is focuses on the basic processes used the for fabrication of passive fiber components i.e., physical tapering and thermal core expansion, while Section 4 describes, in detail, the criteria that should be taken into account during the design of those components. Section 5 summarizes recent achievements in both the design and fabrication of power combiners and mode field adaptors. The various approaches used by research teams in order to increase coupling efficiency, including our own original results, are analyzed and described.

2. Passive Fiber Components—Power Combiners and Mode Field Adaptors

For the needs of all-fiber construction several power combiner schemes were developed, which can be divided into side- and end-pumping methods [18]. Figure 1a,c represents the side-pumping scheme, where, in both cases, the outer clad needs to be grinded down. In the distributed side coupling scheme (Figure 1a) the pump fiber is fused to an active DC fiber on a long section allowing for pumping the active fiber in forward and backward direction simultaneously [19,20]. The scheme presented in Figure 1c represents conventional side-pumping method in an all-fiber construction approach [21–23].

Properly cleaved or polished at some angle pump fiber is attached to the cladding of the DC fiber by fusing or using optical adhesive. Figure 1b shows pumping by fused fiber bundle with tapered bridging fiber. In this case the input fiber bundle is fused and spliced with a bridging (intermediate) fiber which then is tapered down and spliced to an output DC fiber [24]. Figure 1d presents the most common tapered fused bundle (TFB) power combiner scheme, where the input fiber bundle is fused (e.g., after placing it inside the capillary tube), tapered down, cleaved, and spliced to the DC fiber [13–16,25,26]. In the case of the schemes shown in Figure 1b,d, the input fiber bundle can include signal fiber in the center, while in the case of side-pumping approaches signal fiber can be simply spliced to the one of free ends of the active DC fiber.

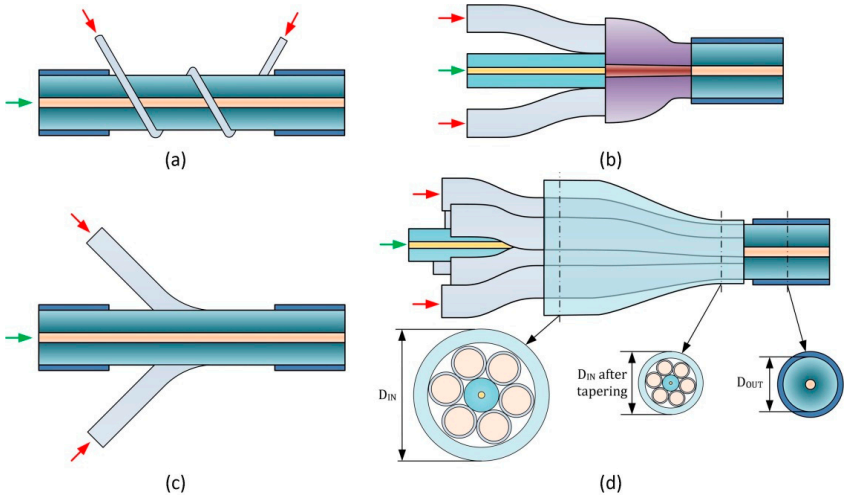

Figure 1. Power combiner realization schemes: Distributed side coupling (**a**), end-pumping through fused fiber bundle and tapered bridging fiber (**b**), conventional side coupling (**c**), and end-pumping through tapered fused fiber bundle (**d**).

There are two basic configurations of TFB power combiners. The pump power combiner in N × 1 configuration consists of only multimode (MM) pump fibers and it is typically used in laser setups. The same N × 1 configuration is used for signal power combiners, where instead, N number of pump fibers signal fibers is used. Those types of power combiners are used for incoherent beam combining. The pump and signal power combiner in (N + 1) × 1 configuration beside pump fibers in the input fiber bundle utilizes also one feed-through signal fiber (SM or LMA) and it is typically used in amplifier setups. As pump ports, combiners typically utilize MM fibers with 105/125 µm core/clad diameter and core numerical aperture (NA) of 0.15 or 0.22. However, nowadays lasers and amplifiers are generating kilowatt power levels, thus MM pump port diameters for such high power operation are significantly higher (e.g., 200 ÷ 400 µm). Typically a DC passive fiber with inner cladding diameter ranging from 125 to 400 µm (depends on the operating optical power level) is used as an output fiber. The input signal fiber can be SM or LMA, same as the output DC fiber.

Typical pump power combiner configuration is 7 × 1 with seven MM fibers (core/clad diameter of 105/125 µm, and an output SM DC fiber of 125 µm inner cladding diameter. This configuration is offered by several manufacturers with pump power coupling efficiency of >90% [27]. A 7 × 1 power combiner with an LMA type output fiber and a greater than 125 µm inner cladding diameter is more common and offers more options regarding to the type of input and output fibers [28]. The most popular configuration in the case of pump and signal power combiner is (6 + 1) × 1. This configuration, with a SM input signal fiber and 125 µm output fiber cladding diameter, is offered, e.g., by Gooch & Housego or Laser Components with transmission efficiencies >90% for 980 nm pump light and >85% for ~1550 nm signal light [29,30]. Commercially available power combiners that utilize an LMA type output fiber with an inner cladding diameter of minimum 250 µm are more common [30,31]. Signal combiners in the N × 1 configuration are available e.g., ITF Technologies offer

3 × 1 configuration with power handling of 3 kW or 6 kW [32], and Laser Components offer 4 × 1 and 6 × 1 configurations with possible power handling of 3 kW, 5 kW, or 10 kW [30].

In a high-power laser or amplifier system one can use different types of fibers (SM and LMA), which have different core and mode field diameters (MFDs), and therefore a more sophisticated fusion splice way for connecting them is needed. Transmission between fibers may be realized by an optical setup (based on bulk optics components); however, since an all-fiber system configuration is more profitable one should use a fiber mode field adaptor (MFA). MFA can be fabricated by simple tapering e.g., a fiber with larger core diameter, in order to match its MFD to a fiber with smaller dimensions. Besides tapering for matching two different mode field diameters, a thermal core expansion can be also used as a single process or in a combination with tapering [33].

For research groups who are working on fiber lasers or amplifiers systems operating with customized fibers it is often a problem to find a commercial power combiner or MFA compatible with fibers used in the setup, hence such components are still being developed by many research teams [34].

3. Basic Power Combiners and Mode Field Adaptors Fabrication Processes

More and more achievements in the field of fabrication of passive fiber components can be continuously found because advanced splicing systems (e.g., 3SAE LDS System, Vytran Fusion Splicing System, or Fujikura Laser Splicing System) are becoming more commonly available. Those systems enable the use of two basic processes for changing fiber properties such as core diameter and clad and mode field: thermal core expansion (TEC) (Figure 2a) and physical tapering (Figure 2b).

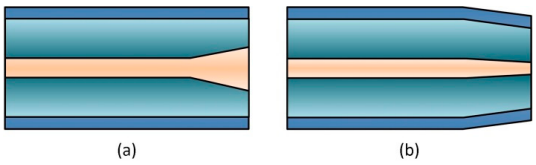

Figure 2. Scheme of changes in optical fibers as a result of thermal core expansion (**a**) and physical tapering (**b**).

TEC is a technology which allows for effective reduction of the mode field mismatch loss between two different fibers [35–39]. This process involves heating fibers with a temperature typical for splicing (for a silica fiber it is approximately 2000 °C) for much longer than a splice itself. Due to heating the dopants from the core are diffusing, enlarging the core diameter and decreasing the refractive index difference between the core and clad, resulting in the MFD increase. This process should not cause the clad diameter to increase; however, heating a fiber for too long can cause its deformation [40]. TEC does not change the V-number defined as [41]:

$$V = \frac{2\pi}{\lambda} rNA, \tag{1}$$

where λ—wavelength, r—core radius, numerical aperture $NA = n_0\sqrt{n_1^2 - n_2^2}$ (n_1, n_2—core and clad refractive index). V—number remains constant, because changes in core diameter and NA are compensating each other (while core radius grows, NA decreases). This means that the SM fiber will remain an SM fiber.

Physical tapering has different effects. Here the refractive index difference is constant, while clad and core diameters are reduced. This changes the V-number, therefore the MFD is also changed. The fiber mode field radius (r_{mode}) for SM fibers with a step index profile can be calculated using the Marcus equation [42]:

$$\frac{r_{mode}}{r} \approx 0.65 + \frac{1.619}{V^{3/2}} + \frac{2.879}{V^6}, \tag{2}$$

The above equation is precise for $V > 1$ however, for SM fibers characterized as $V < 2.405$, and also for LMA type fibers (when $V > 2.405$), this equation refers to their fundamental mode. Figure 3 shows the impact of the fiber core diameter change on MFD for two signal wavelengths (1550 nm and 2000 nm) and for a various number of common fibers NA operating on those wavelengths.

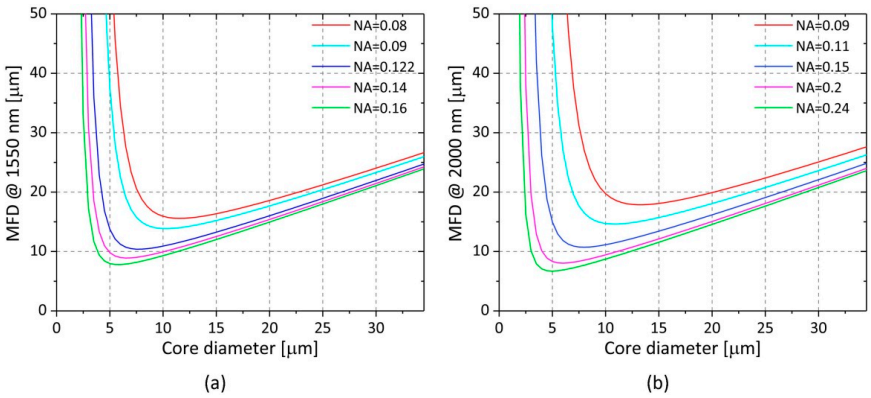

Figure 3. MFD change depending on the core diameter change, calculated for 1550 nm (**a**) and 2000 nm (**b**) wavelength and for different numerical apertures (NAs).

As it can be seen from Figure 3, when the core diameter decreases and NA is constant, the MFD change has a hyperbolic paraboloid shape, and it decreases while the core diameter is reduced; however, for certain NA there is a value of the core diameter below which the MFD stars to grow very rapidly. This analysis shows that tapering a fiber to a core diameter that is too small could give the opposite effect from the intended one. Tapering a fiber will reduce its MFD only to a certain core diameter, below which the MFD will increase very rapidly.

4. Basic Criteria and Limits for Optical Fiber Tapering Process

During fabrication of a MFA or power combiner, physical tapering may cover signal fibers as well as pump fibers. In order to achieve the best signal and pump power transmission efficiency through tapered fibers, light leakage from their cores needs to be avoided; this is a huge challenge considering the fiber core diameter decrease caused by physical tapering. Any leakage of light inside the component will cause transmission loss in the whole system in which it is applied. Additionally, while operating in a high-power regime, such leakage of high-power light might cause local overheating and damage the structure, which can have a destructive influence on the setup. In order to avoid those problems, and maintain the high-transmission efficiency of light propagated through the tapered fiber, certain criterion must be fulfilled [18,40].

4.1. Adiabatic Criterion for Single Mode Fiber Tapering

In the case of SM signal fibers which have very small core diameter (typically 6–10 μm), the basic rule is that a taper should be characterized by a gradual and slow core diameter decrease, which can be expressed as

$$\frac{\Delta r}{r} \ll 1, \tag{3}$$

where Δr—core diameter change and r—initial core diameter. Too rapid a change of the core diameter will cause coupling of the optical power from the fundamental mode into the fiber higher order modes (HOM) [43]. One can assume that the taper diameter change is slow and gradual, until the fiber radius change (Δr) is small relative to the beat length (L_B) between the fundamental mode and first of the HOM [18,41,44,45]. The local change of fiber core radius relative to the beat length can be expressed as:

$$\Delta r = L_B \frac{dr}{dz}, \tag{4}$$

where dr/dz describes the change of the radius (dr) on the length (dz). The beat length between the fundamental mode and HOM is expressed by $L_B = 2\pi/(\beta_1 - \beta_2)$, where β_1 and β_2 are the propagation constants of the fundamental mode (LP_{01}) and the first HOM, respectively. The propagation constant is expressed as $\beta = n_{eff}2\pi/\lambda$ (n_{eff}—effective refractive index and λ—wavelength). By inserting Equation (4) into Equation (3) we get the adiabatic criterion for tapering single mode fibers:

$$\frac{dr}{dz} \leq \frac{r}{L_B}, \tag{5}$$

Taking β_2, the propagation constant of the first HOM, which is the closest one to the propagation constant of the fundamental mode (β_1), the L_B will be at maximum value and the adiabatic criterion will be more strict. By fulfilling the above criterion the transmission loss in the tapered fiber should be minimal [18]. For a linear taper profile the taper slope (dr/dz) will be constant on entire taper length, thus it can be assumed that $dz = L$ and $dr = r_1 - r_2$, where r_1 represents the core radius before tapering, and r_2 represents the core radius after tapering giving

$$\frac{r_1 - r_2}{L} \leq \frac{r}{L_B}, \tag{6}$$

From Equation (6) we can calculate the minimum taper length fulfilling the adiabatic criterion. In order to obtain the largest value of L one should take as a fiber core radius (r), radius after tapering (i.e., $r = r_2$). Additionally, the taper ratio can be written as $TR = r_1/r_2$, thus the adiabatic criterion from Equation (6) can be finally reduced to

$$L \geq (TR - 1)L_B, \tag{7}$$

where L define the minimal taper length for which it will be adiabatic [18].

4.2. Brightness Ratio and Adiabatic Criterion for Multimode Fiber Tapering

During the fabrication of power combiners the tapering process also covers MM fibers with a much larger core diameter in comparison with SM fibers, and with a much larger number of excited modes, thus the adiabatic criterion from Equation (5) is not suitable for these kinds of fibers. In order to avoid significant losses, the beam brightness, proportional to transmitted optical power, should be preserved [14,41,46]. The brightness ratio (BR) parameter allows us to estimate the transmission loss of the designed combiner, and it can be designated as follows:

$$\left(\frac{NA_{out}}{NA_{in}}\right)^2 \geq \frac{nP_{in}}{P_{out}}, \tag{8}$$

where n defines number of input pump fibers, NA_{in} and NA_{out} defines numerical apertures of input fibers and output fiber, and P_{in}, P_{out} describes the cross sectional area of single input fiber and an output fiber. After the appropriate transformations and change of the cross sectional areas into the diameters of the considered fibers, the above criterion is transformed into the BR parameter [47]:

$$BR \approx \frac{D_{out}^2 NA_{out}^2}{nD_{in}^2 NA_{in}^2} \geq 1, \tag{9}$$

where D_{out} and D_{in} are the diameters of output and input fibers. If $BR \geq 1$, then the beam brightness is preserved, which means that the beam intensity launched into n pumping ports is equal to the intensity of the beam at the combiner output. $BR < 1$ means a loss of the beam brightness (beam intensity at the output is lower than at the input), which may be caused by, for example, the leaking of the beam from the structure.

Similar as in case of SM fibers, there is also adiabatic criterion for MM fibers; however, since in that case we are dealing with much larger number of excited modes, we are assuming that the core radius change should be sufficiently small regarding to the half ray period—Z_P (Figure 4) [41].

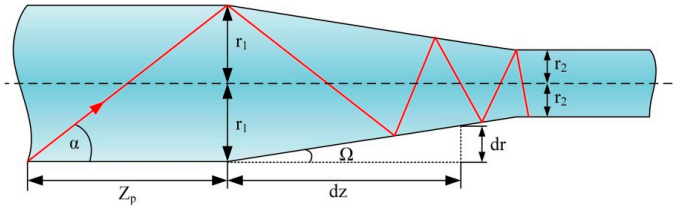

Figure 4. Scheme of ray propagation in a multimode fiber, adapted from [18,41].

Adiabatic criterion for MM fibers is defined as follows:

$$\frac{dr}{dz} \leq \frac{r}{Z_P}, \tag{10}$$

For a given $NA = sin(\alpha)$, a ray that passes through the optical axis of the fiber will have the longest half ray period: $Z_P = 2r/tan\,\alpha$. In case of a linear taper shape ($dr = r_1 - r_2$ and $dz = L$) the adiabatic criterion can be transformed into an equation which will give the minimum taper length for which the taper will be adiabatic:

$$L \geq \frac{2(r_1 - r_2)}{tan\,\alpha} = \frac{D_1 - D_2}{tan\,\alpha}, \tag{11}$$

Another criterion whose fulfillment guarantees the MM fiber taper will be adiabatic, occurs when the local angle Ω (defined by dr/dz in Figure 4) is equal to or smaller than the half of the ray angle α [18,41].

5. Recent Achievements in the Field of Designing and Fabrication of High-Power Components

In this section recent achievements in the designing and fabrication of mode field adaptors and power combiners are described. Configurations include pump, pump and signal, and only signal coupling; they are characterized by the signal and/or pump radiation coupling efficiency. These components use different types of fibers that are fabricated in various configurations and in different fabrication processes.

5.1. Pump Power Combiners

The pump power combiner in N × 1 configuration is used when N pump sources (typically with an MM fiber) have to be combined into one output fiber [17,25,47–50]. The lack of a feed-through signal fiber simplifies the design and fabrication process of this component. The most recent achievements are presented in Table 1. The 7 × 1 configuration seems to be the most common approach, but lower or higher numbers of pump ports can also be found.

Table 1. Summary of recently reported pump power combiners [51–57].

Config.	Input Pump Fiber, Core NA	Output DC Fiber, Clad NA	Pump Transmission Efficiency	Year/Ref.
7 × 1	105/125 µm, NA = 0.22	30/250 µm, NA = 0.46	98.9%	2016/[51]
7 × 1	Core ϕ = 110 µm, NA = 0.22	20/400 µm, NA = 0.46	~80%	2010/[52]
7 × 1	105/125 µm, NA = 0.22	9/125 µm, NA = 0.46	~80%	2015/[53]
7 × 1	220/242 µm, NA = 0.22	20/400 µm, NA = 0.46	98.4%	2015/[54]
7 × 1	200/220 µm, NA = 0.22	400/550 µm, NA = 0.46	99.4%	2016/[55]
3 × 1	200/220 µm, NA = 0.22	400/440 µm, NA = 0.22	95.1%	
16 × 1	105/125 µm, NA = 0.15	200/220 µm, NA = 0.46	93%	2013/[56]
32 × 1	105/125 µm, NA = 0.15	20/400 µm, NA = 0.46	92.8%	2008/[57]

An interesting approach for improving pump power transmission efficiency using a capillary tube with refractive index matching the refractive index of the clad of the MM fiber was presented in [51]. The capillary tube acts as a clad of MM fibers and helps to keep the radiation inside the fiber bundle. This allows for the achieving of higher pump transmission efficiency compared to the combiners in which the refractive index of the capillary tube matches the refractive index of the MM fiber core. In this second case, the radiation leaks out from the fiber into the capillary causing additional transmission losses.

Another critical parameter in power combiner fabrication is the ratio between the diameters of the input fiber bundle and the output fiber. When input and output fibers with large core and clad diameters are used a small taper ratio (TR) is needed, which makes it easier to preserve the brightness of the pump light. However, it is often required to use larger TR. For example, when an output port is a DC fiber with a clad diameter of only 125 µm and seven MM 105/125 µm fibers are used at the input, then the required TR is 3. Presented in our previous work [53] power combiner requiring TR twice as large as presented power combiner in [51], had BR below 1, which indicates losses resulting from the tapering of the input fiber bundle from the initial 375 µm diameter to the diameter of the output DC fiber (125 µm). Using input and output fibers with much larger clad diameters [51,52,54–57] helps to maintain high beam brightness and achieve handling of a very large amount of pump power. In a paper [55] two configurations of power combiners are presented: 3 × 1 and 7 × 1 capable to handle approximately 2.1 kW and 4.72 kW, respectively.

It is challenging to design and fabricate a power combiner with relatively small cladding diameter of the output fiber, and it is also challenging to combine more than ten input fibers in the bundle. In a paper [56] a 16 × 1 power combiner was fabricated by double bundling of the input fibers. Scheme of the fabrication process is presented in Figure 5a. A 32 × 1 power combiner has been demonstrated in [57]. In this case, the input fiber bundle not only has 32 pump ports, but also an additional large central fiber which is used to guide the Amplified Spontaneous Emission (ASE) light and unwanted back reflections from other parts of the setup.

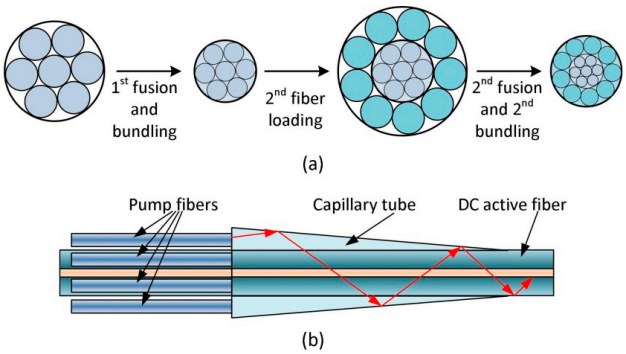

Figure 5. Scheme of double bundling process for fabrication of 16 × 1 power combiner adapted from a paper [56] (**a**) and a side-pump power combiner in 7 × 1 configuration adapted from a paper [52] (**b**).

An interesting design described in [52] uses a 7 × 1 power combiner with a side-pumping approach. Comparing to the other power combiners presented in this subsection, its fabrication process is quite sophisticated. The DC fiber is placed and fused in the capillary tube whose outer diameter decreases in the output direction (this was achieved by hydrofluoric acid bath). Subsequently, MM fibers are spliced to the front side of the capillary tube (with larger diameter, as shown in Figure 5b). In this configuration the capillary tube with gradually decreasing outer diameter plays the role of additional cladding layer for the DC fiber.

5.2. Pump and Signal Power Combiners

The design and fabrication process of pump and signal combiners is far more challenging than in the case of pump power combiners, because, besides pump power being transmitted from tapered MM

fibers into the inner cladding of the output DC fiber, there is also a signal fiber, which tapering decreases its initially small core diameter. This may result in its mode field mismatch with the output fiber, and thus significant signal transmission losses. Many scientific reports presenting theoretical modeling and fabrication of those kind of components can be found in the literature [58–63]. A (6 + 1) × 1 configuration is the most common configuration of pump and signal power combiner. However, as in the case of pump power combiners, in this type of power combiner different configurations with a lower or higher number of pump ports can be found in the literature. The dimensions and number of input fibers must be arranged in a way that the signal feed-through fiber is placed in the center surrounded by pump fibers. Some recently presented fabricated pump and signal power combiners are shown in Table 2.

Table 2. Summary of recently reported pump and signal power combiners [16,64–72].

Config.	Input Signal Fiber, Core/Clad NA	Input Pump Fiber, Core NA	Output DC Fiber, Core/Clad NA	Signal/Pump Transmission Efficiency	Year/Ref.
(4 + 1) × 1	25/250 µm, NA = 0.06/0.46	Core ϕ = 105 µm, NA = 0.22	25/250 µm, NA = 0.06/0.46	97/90%	2013/[64]
(5 + 1) × 1	9/80 µm, NA = 0.13	105/125 µm, NA = 0.22	9/125 µm, NA = 0.122/0.46	94.5/91%	2017/[65]
(6 + 1) × 1	8.2/125 µm, NA = 0.14	105/125 µm, NA = 0.15	25/250 µm, NA = 0.6/0.46	94/96–99%	2015/[66]
(6 + 1) × 1	6–10/125 µm, NA = 0.14	105/125 µm, NA = 0.15–0.22	25/250 µm, NA = 0.06/0.46	94/94%	2011/[16]
(6 + 1) × 1	DC PM 20/400 µm, NA = 0.065/-	200/240 µm, NA = 0.22	DC PM 20/400 µm, NA = 0.065/-	91/~99.8%	2014/[67]
(6 + 1) × 1	DC 20/400 µm, NA = 0.06/0.46	200/220 µm, NA = 0.22	20/400 µm, NA = 0.06/0.46	97.7/98%	2017/[68]
(6 + 1) × 1	DC 30/220 µm, NA = 0.06/-	200/220 µm, NA = 0.22	30/600 µm, NA = 0.06/-	~99.8/94.8%	2018/[69]
(6 + 1) × 1	10/125 µm, NA = 0.08/0.46	105/125 µm, NA = 0.22	20/400 µm, NA = 0.06/0.46	87.52/98.6%	2017/[70]
(7 + 1) × 1	SM PM MFD = 15 µm, clad ϕ = 160 µm, NA = 0.06/-	105/125 µm, NA = -	SM PM MFD = 15 µm, clad ϕ = 133 µm, NA = 0.06/-	~85/~94.5%	2010/[71]
(8 + 1) × 1	100/200 µm, NA = 0.054/0.46	105/125 µm, NA = 0.15	100/400 µm, NA = 0.054/0.46	98/96.8%	2013/[72]

One of the approaches to preserve high signal transmission is fabrication of the power combiner in a side-pumping scheme. An example of this type of combiner in (4 + 1) × 1 configuration is presented in a paper [64]. Here, each pump fiber was spliced to an intermediate coreless fiber, which was then fused around the passive DC fiber (Figure 6a). In this approach, minimal impact from the fabrication process on the signal fiber is guaranteed.

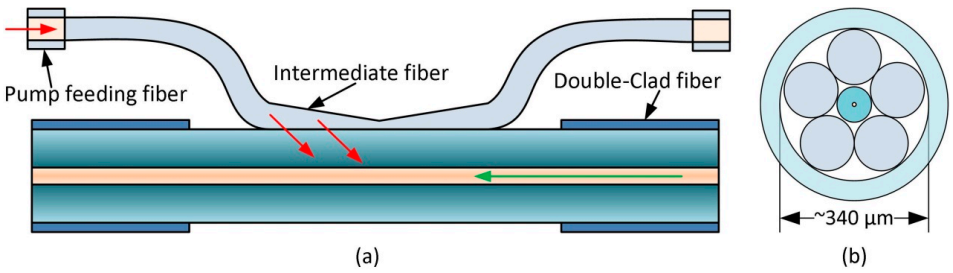

Figure 6. Scheme of the side-pump power combiner adapted from a paper [64] (**a**) and the cross sectional area of (5 + 1) × 1 power combiner adapted from our previous work [65] (**b**).

More often than not power combiners are fabricated in an end-pumping scheme by a TFB technology. As it can be seen in Table 2, power combiners with output DC fibers diameter of below 200 µm are not very common. This is because they require high TR, which makes it very difficult to preserve high pump power and signal coupling efficiency due to the loss in beam brightness and MFD mismatch of signal input fiber with output fibers. In our previous work [65], a power combiner in an (5 + 1) × 1 configuration is presented with an output SM DC passive fiber with inner cladding diameter of only 125 µm. To improve signal transmission efficiency we have used five pump fibers (instead of six) and signal feed-through fiber with lower clad diameter of 80 µm than commonly used 125 µm (Figure 6b). This allowed us to decrease the TR and achieve signal transmission on the level of 94.5%. In a paper [71] a (7 + 1) × 1 configuration is reported with 133 µm diameter of the output DC fiber, and with 160 and 125 µm clad diameter of the input signal and pump fibers, respectively. It is an example of a power combiner with DC photonics crystal fibers (PCFs). Here eight input fibers were only fused together to form a bundle. As an output fiber an SM PM DC fiber with MFD = 15 µm with an air-cladding was chosen. In order to match the input fiber bundle with the output fiber an intermediate PCF fiber was used, on which tapering was performed.

(6 + 1) × 1 power combiners utilizing single mode input signal fibers, 105/125 µm pump fibers and a 25/250 µm DC fiber at the output are presented in papers [16,66]. In paper [66] a conventional SMF28e fiber is used as a feed-through fiber and the signal transmission efficiency was improved from 51% to 94% thanks to the TEC technique. In a paper [16], the authors reported a signal and pump power transmission efficiency of 94%. In this case, the custom-made fixture was used for power combiner fabrication, and the authors pointed out that the fabrication process may include etching of fibers, thus decreasing their clad diameter without any impact on their core.

Another interesting approach to achieve high signal transmission efficiency is presented in paper [67]. With vanishing core technology the authors developed a polarization maintaining (6 + 1) × 1 power combiner with a signal and pump power transmission efficiency of 91% and 98%, respectively. In this method before the tapering process the initial mode field is determined by the refractive index difference of n_1 (of the "vanishing" core) and n_2 (of the secondary core) as it was explained by the authors [67] (Figure 7a). After tapering, the central core is too small to guide the light, thus we may assume that it vanished. Therefore, at the taper output the mode field is determined by the refractive index difference of the second and third layers (n_2 and n_3, respectively). In order to use this method a special signal fiber with an additional layer of the secondary core must be used.

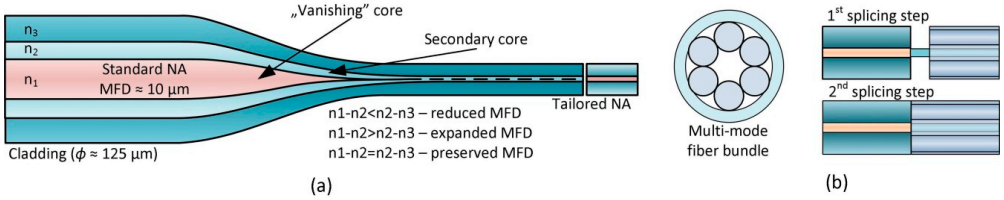

Figure 7. Cross-section of the refractive index profile along a signal fiber taper with the vanishing core technology adapted from a paper [67] (**a**); stages of (6 + 1) × 1 combiner fabrication process adapted from a paper [68]: cross-section of MM fiber bundle (left), 1st splicing step (upper right) and 2nd splicing step (bottom right) (**b**).

High signal and pump transmission of more than 97% and 98%, respectively, was achieved in a paper [68]; the same signal fiber was used in the input fiber bundle and at the output of the (6 + 1) × 1 combiner. Such high transmission efficiency was possible due to the reduced input signal fiber cladding by the chemical corrosion and two-step splicing method. The fabrication process differs from that previously presented. At first six pump fibers were placed in the capillary tube and contacted with its wall forming a ring shape. Then, the bundle was tapered down creating an approximate hexagon hole in the middle with a diameter of approximately 100 µm. A scheme of the cross sectional area of the bundle is presented in Figure 7b (left image). The clad of the input signal fiber was reduced

to less than 100 µm by chemical corrosion. Then the signal fiber was inserted into the hole of previously prepared bundle. Two-step splicing meant that, at first, the signal fiber from the bundle was spliced with the output fiber (Figure 7b, upper right image) and then the rest of the bundle—pump fibers were moved to the output fiber and carefully fused and spliced (Figure 7b, bottom right image).

In a paper [69] a (6 + 1) × 1 power combiner was designed in a way that the input fiber bundle diameter is only slightly larger than the output fiber diameter. Authors have used home-made signal fibers at the input and output with core/clad diameter of 30/220 µm and 30/600 µm, respectively. In their design, signal fibers have the same core diameter, and the combiner fabrication only requires fusing of the input fiber bundle, without the tapering, resulting in a small change of the input signal fiber core and very high signal transmission efficiency.

Another unconventional (8 + 1) × 1 configuration was presented in [72]. Just like in the case of power combiners with an output DC fiber diameter of 400 µm and above, very high signal transmission efficiency was achieved; however, the signal and output fibers were characterized with a very large core diameter of 100 µm. The fabrication process developed by the authors is slightly similar as in a paper [68]. Here, eight pump fibers are arranged in a ring configuration by holding clamps and a pretaper process is performed on them, reducing the diameter of each MM fiber from 125 to 100 µm. Then, the input signal fiber is inserted into the middle of the pretapered bundle, pump fibers are slightly twisted around the signal fiber for better attachment, and then the whole structure is fused, cleaved, and spliced to the output fiber. As it was described in this case, as well as in the papers [16,68], the input signal fiber is not tapered down, but it is inserted into the properly prepared input fiber bundle and/or its decreased clad diameter is achieved by chemical etching, resulting in very high signal transmission efficiency.

Another interesting approach applies a built-in mode field adaptor [14,60,61]. Such a solution was chosen by authors of a work [70] however, an intermediate fiber was not used. Here the input fiber bundle and the output DC fiber were both tapered down in order to match their mode fields. Then they were spliced, resulting in a transmission efficiency above 87% and 98% of the signal and pump power, respectively.

5.3. Signal Power Combiners

Currently the output power of fiber lasers have reached the kilowatt (kW) level however, phenomena such as thermal damage, nonlinear effects and modal instabilities limit the power level at the output of a single fiber laser. An interesting and relatively simple solution uses a beam combining technique by merging the output power of several hundred watts (from several lasers) into one large core delivery fiber [26,50–79]. Incoherent beam-combining based on fiber technology is particularly interesting because it allows preserving all the advantages of the all-fiber laser construction technique. Recently presented signal power combiner are shown in Table 3.

Table 3. Summary of recently reported signal power combiners [80–83].

Config.	Input Fibers, Core/Clad NA	Output Fiber, Core NA	Signal Transmission Efficiency, M^2, Power Handling	Year/Ref.
7 × 1	SM 17/125 µm, NA = -	MM 100/660 µm, NA = 0.22	94.7%, M^2 = 6.5, 2.5 kW	2011/[80]
3 × 1	30/125 µm, NA = 0.08/0.46	100/360 µm, NA = 0.2	>96%, M^2 = 1.2/1.3, >200 W	2015/[81]
7 × 1	20/130 µm, NA = 0.08/0.46	50/70/360 µm, NA = 0.22	98%, M^2 = 4.3, 6.26 kW	2016/[82]
7 × 1	20/400 µm, NA = 0.06	50/70/360 µm, NA = 0.22	>98.5%, M^2 = 5.37, >10 kW	2018/[83]

LMA type fibers are typically used as input fibers in signal power combiners. As an example of such configuration a 7 × 1 signal power combiner capable of handling a 2.5 kW signal power with M^2 = 6.5 was presented in paper [80]. Another7 × 1 power combiner presented in [82], shows the development and transmission efficiency scaling of combiners presented by the same research group in papers [76,84]. In a combiner reported in [84], the output fiber had a 100 µm core diameter, resulting in signal transmission on the level of ~99%, $M^2 \approx 10$ and measured power handling of about 500 W. In a paper [76] the output fiber core diameter was 2-fold smaller (50 µm), and the signal transmission efficiency was at the same level as previously however, the M^2 factor was improved (M^2 = 6.0/6.3). In all the above-presented and discussed signal power combiners by this research group the same signal fibers were used as inputs: 20/130 µm (NA = 0.08/0.46) [76,82,84]. With smaller output fiber core diameter they were able to achieve ~99% signal transmission efficiency with M^2 = 6.0/6.3 [76], and later [82] 98% signal transmission efficiency with improved M^2 = 4.3 and measured power handling of 6.26 kW. In these papers a fluorine-doped low-index capillary was used, forming with input fibers a structure with seven cores and a cladding created by low-index capillary tube. In a recent report [83] a 7 × 1 power combiner achieved power handling of above 10 kW with measured M^2 = 5.37 (at 14 kW of the output power). In this case the authors used input fibers with much larger cladding diameter (400 µm); this diameter can be decreased by chemical etching. The signal power combiner fabricated in 3 × 1 configuration presented in [81] was used to incoherently combine a supercontinuum source with power above 200 W. Because photonic crystal fibers have unique features which classical fibers do not have (e.g., high birefringence, larger single-mode areas, extremely low/high nonlinearity, and, in the case of hollow-core PCF, high damage threshold), therefore it is profitable to use PCF in components operating at high-power kW regimes; some theoretical and experimental achievements in this field have already been reported [85–87].

5.4. Mode Field Adaptors

Mode field adaptors are not that complicated in fabrication as power combiners however, they are equally important in all-fiber MOPA configurations. A MFA may even be considered as a splice between two fibers with slightly different mode field diameters. Typically, they are fabricated just like power combiners by tapering or TEC method or the combination of both [88–91] however, there are other solutions like mode field adaptors based on multimode interference in graded index multimode fiber (GIMF) [92,93].

In most cases presented in Table 4 the authors have used, not only the TEC method, but they have combined it with the tapering process. Using each method separately will not give a mode field match as precise as they can achieve when combined together [91]. This is why the authors of a paper [91] were able to achieve approximately 95% signal transmission efficiency, despite a very large core and mode field diameter difference of used fibers. Two configurations of MFA, where at the input the authors have used firstly a 4/125 µm SM fiber, and secondly a 5/125 µm SM fiber, while a 15/130 µm LMA fiber was used as the output (in both cases) [94]. The MFAs achieved signal transmission efficiency of approximately 93% and 91%, respectively, with only the TEC method used for fabrication process. The same research group presented two MFAs with the same input fibers [95]; however, as an output fiber they have used a 25/250 µm LMA fiber with a larger MFD than in the previous case. Here the LMA fiber has MFD = 21.5 µm, while in the previous work the LMA fiber had MFD = 13.6 µm. This means much larger mode field mismatch with the input fiber, thus authors have used here TEC method combined with the tapering, which allowed to achieve signal transmission efficiency on level of >90%. In our most recent work, reported recently [96], two types of MFAs are mentioned. The first one connects two types of double clad LMA fibers, thus it guide both the signal and pump power with an efficiency of 92%. In the case of this MFA we have used only tapering in the fabrication process; however, in the case of the second MFA, we combined tapering with the TEC method. It was necessary to use both methods because of the large mode field mismatch of used fibers.

Table 4. Summary of recently reported mode field adaptors [91,94–96].

Input Fiber, Core NA	Output Fiber, Core NA	Signal Transmission Efficiency	Year/Ref.
5.3/125 µm, NA = 0.14, (Corning Hi1060)	20/400 µm, NA = 0.06	~95%	2007/[91]
4/125 µm, NA = 0.2, (HI1060FLEX)	15/130 µm, NA = 0.08	~93%	2013/[94]
5/125 µm, NA = 0.14, (HI1060)	15/130 µm, NA = 0.08	~91%	
4/125 µm, NA = 0.2, (HI1060FLEX)	25/250 µm, NA = 0.06	>90%	2014/[95]
5/125 µm, NA = 0.14, (HI1060)	25/250 µm, NA = 0.06	~90%	
20/200 µm, NA = 0.08	25/300 µm, NA = 0.09	92%	2018/[96]
8.2/125 µm, NA = 0.14	20/130 µm, NA = 0.08	90%	

6. Summary

In conclusion, passive fiber components (i.e., power combiners and mode field adaptors) are key components in a very beneficial all-fiber configuration of laser and amplifier setups. Their precise design and fabrication is very important for achieving low-loss transmission, which will allow the constructing of highly efficient and reliable fiber setups of lasers or amplifiers operating in high power regime. Two main fabrication processes (tapering and thermal core expansion) and their impact on the optical fiber have been described. Basic adiabatic criteria and brightness ratio parameters have been explained in detail. The most important and impressive achievements in the field of design and fabrication of passive fiber components to be discovered recently, like power combiners and mode field adaptors, have been summarized and described. As it can be seen, many research teams are still developing designs as well as fabrication processes (basing on tapering and TEC process) in order to achieve high coupling efficiency of customized components.

Funding: This research was funded by National Science Centre (decision No. UMO-2015/19/N/ST7/01511).

Acknowledgments: D.S. would like to acknowledge the support from the National Science Centre (NCN), Poland under the project "Pump and signal power combiner with improved signal transmission efficiency" (decision No. UMO-2015/19/N/ST7/01511). The author expresses her thanks to the members of the Laser Sensing Laboratory Group (Michal Nikodem and Piotr Jaworski) for their help and valuable discussions.

Conflicts of Interest: The author declare no conflicts of interest.

References

1. Philippov, V.; Codemard, C.; Jeong, Y.; Alegria, C.; Sahu, J.K.; Nilsson, J.; Pearson, G.N. High-energy in-fiber pulse amplification for coherent lidar applications. *Opt. Lett.* **2004**, *29*, 2590–2592. [CrossRef] [PubMed]
2. Codemard, C.; Farrell, C.; Dupriez, P.; Philippov, V.; Sahu, J.K.; Nilsson, J. Millijoule, high-peak power, narrow-linewidth, subhundred nanosecond pulsed fibre Master-Oscillator Power- Amplifier at 1.55 µm. *Comptes Rendus Phys.* **2006**, *7*, 170–176. [CrossRef]
3. Dolfi-Bouteyre, A.; Canat, G.; Valla, M.; Augere, B.; Besson, C.; Goular, D.; Lombard, L.; Cariou, J.P.; Durecu, A.; Fleury, D.; et al. Pulsed 1.5 µm LIDAR for axial aircraft wake vortex detection based on high brightness large-core fiber amplifier. *IEEE J. Sel. Top. Quantum Electron.* **2009**, *15*, 441–450. [CrossRef]
4. Braglia, A.; Califano, A.; Liu, Y.; Perrone, G. Architectures and components for high power CW fiber lasers. *Int. J. Mod. Phys. B* **2014**, *28*, 1442001. [CrossRef]
5. Filippov, V.; Chamorovskii, Y.; Kerttula, J.; Golant, K.; Pessa, M.; Okhotnikov, O.G. Double clad tapered fiber for high power applications. *Opt. Express* **2008**, *16*, 1929–1944. [CrossRef] [PubMed]
6. Snitzer, E.; Po, H.; Hakimi, F.; Tuminelli, R.; McCollumn, B.C. Double-clad, offset core Nd fiber laser. *OSA Proc. Opt. Fiber Sens.* **1988**, *2*. [CrossRef]
7. Goldberg, L.; Cole, B.; Snitzer, E. V-groove side-pumped 1.5 µm fiber amplifier. *Electron. Lett.* **1997**, *33*, 2127–2129. [CrossRef]
8. Swiderski, J.; Zajac, A.; Skorczakowski, M. Pulsed ytterbium-doped large mode area double-clad fiber amplifier in MOFPA configuration. *Opto-Electron. Rev.* **2007**, *15*, 98–101. [CrossRef]
9. Raring, J.W.; Coldren, L.A. 40-Gb/s Widely Tunable Transceivers. *IEEE J. Sel. Top. Quantum Electron.* **2007**, *13*, 3–14. [CrossRef]

10. Richardson, D.J.; Nilsson, J.; Clarkson, W.A. High power fiber lasers: Current status and future perspectives. *J. Opt. Soc. Am. B* **2010**, *27*, B63–B92. [CrossRef]
11. Gapontsev, V.P.; Samartsev, L.E. High-power fiber laser. *OSA Proc. Adv. Solid State Lasers* **1990**, *6*. [CrossRef]
12. Shi, W.; Fang, Q.; Zhu, X.; Norwood, R.A.; Peyghambarian, N. Fibre lasers and their applications [Invited]. *Appl. Opt.* **2014**, *53*, 6554–6568. [CrossRef] [PubMed]
13. Gonthier, F.; Martineau, L.; Azami, N.; Faucher, M.; Seguin, F.; Stryckman, D.; Villeneuve, A. High-power all-fibre components: The missing link for high-power fibre lasers. *Proc. SPIE* **2004**, *5335*. [CrossRef]
14. DiGiovanni, D.J.; Stentz, A.J. Tapered Fiber Bundles for Coupling Light into and Out of Cladding-Pumped Fiber Devices. U.S. Patent 5,864,644, 26 January 1999. Available online: https://patentimages.storage.googleapis.com/a9/94/bb/7cd3fbe58cd27c/US5864644.pdf (accessed on 3 September 2018).
15. Kosterin, A.; Temyanko, V.; Fallahi, M.; Mansuripur, M. Tapered fiber bundles for high power applications. In Proceedings of the Technical Digest, Optical Fiber Communication Conference, Anaheim, CA, USA, 6–11 March 2005. [CrossRef]
16. Braglia, A.; Olivero, M.; Neri, A.; Perrone, G. Fabrication of pump combiners for high power fibre lasers. *Proc. SPIE* **2011**, *7914*. [CrossRef]
17. Holland, W.R. All Pump Combiner with Cladless Inputs. U.S. Patent 9,322,993 B1, 26 April 2016. Available online: https://patentimages.storage.googleapis.com/db/f5/e5/a72053d111d362/US9322993.pdf (accessed on 3 September 2018).
18. Noordegraaf, D.; Lægsgaard, J.; Broeng, J.; Skovgaard, P.M.W. *Fused Combiners for Photonic Crystal Fibers. Kgs*; Technical University of Denmark (DTU): Lyngby, Denmark, 2012; 114p, Available online: http://orbit.dtu.dk/files/51271178/2012_01_02_PhD_Thesis_DNO.pdf (accessed on 3 September 2018).
19. Grudinin, A.B.; Payne, D.N.; Turner, P.W.; Nilsson, L.J.A.; Zervas, M.N.; Ibsen, M.; Durkin, M.K. Multi-Fibre Arrangements for High Power Fibre Lasers and Amplifiers. U.S. Patent 6,826,335 B1, 30 November 2004. Available online: https://patentimages.storage.googleapis.com/49/ed/d2/ee2a41c11e4f73/US6826335.pdf (accessed on 3 September 2018).
20. Norman, S.; Zervas, M.; Appleyard, A.; Skull, P.; Walker, D.; Turner, P.; Crowe, I. Power scaling of high power fiber lasers for micromachining and materials processing applications. *Proc. SPIE* **2006**, *6102*. [CrossRef]
21. Gapontsev, V.; Samartsev, I. Coupling Arrangement between a Multi-Mode Light Source and an Optical Fiber through an Intermediate Optical Fiber Length. U.S. Patent 5,999,673, 7 December 1999. Available online: https://patentimages.storage.googleapis.com/b3/5d/29/390f769901abd7/US5999673.pdf (accessed on 3 September 2018).
22. Hakimi, F.; Hakimi, H. A new side coupling method for double clad fiber amplifiers. *Conf. Lasers Electron.-Opt.* **2001**. [CrossRef]
23. Sintov, Y.; Tikva, P. Optical Apparatus. U.S. Patent 2006/0133731 A1, 22 June 2006. Available online: https://patentimages.storage.googleapis.com/16/ce/bd/20d754f19740e2/US20060133731A1.pdf (accessed on 3 September 2018).
24. Nakai, M.; Shima, K.; Saito, M.; Kitabayashi, T. 30W Q-SW fiber laser. *Proc. SPIE* **2007**, *6453*. [CrossRef]
25. Kosterin, A.; Temyanko, V.; Fallahi, M.; Mansuripur, M. Tapered fiber bundles for combining high-power diode lasers. *Appl. Opt.* **2004**, *43*, 3893–3900. [CrossRef] [PubMed]
26. Séguin, F.; Wetter, A.; Martineau, L.; Faucher, M.; Delisle, C.; Caplette, S. Tapered fused bundle coupler package for reliable high optical power dissipation. *Proc. SPIE* **2006**, *6102*. [CrossRef]
27. Gooch & Housego, Multimode Power Combiner. Available online: https://goochandhousego.com/wp-content/uploads/2018/02/GH-DS-FO-TFB-Multimode-Power-Combiner.pdf (accessed on 3 September 2018).
28. ITF Technologies, 3 × 1, 4 × 1, 7 × 1 and 19 × 1 High Power Pump Combiners. Available online: http://www.itftechnologies.com/files/13/JR_ITF_DataSheet_D_3x1_4x1_7x1_19x1_v6_2018-06-06-09-59.pdf (accessed on 3 September 2018).
29. Gooch & Housego, Multimode Power Combiner with Signal Feedthrough. Available online: https://goochandhousego.com/wp-content/pdfs/PEC_0131i3_Multimode_Power_Combiner_with_Signal_Feedthrough.pdf (accessed on 3 September 2018).
30. Laser Components, LIGHTEL, Pump Combiners and Other Optical Components for High Power Fiber Lasers. Available online: https://www.lasercomponents.com/de/?embedded=1&file=fileadmin/user_upload/home/Datasheets/lightel/pump-combiners.pdf&no_cache=1 (accessed on 3 September 2018).

31. ITF Technologies, (6 + 1) × 1 and (18 + 1) × 1 High Power Pump and Signal Combiners. Available online: http://www.itftechnologies.com/files/13/11_DataSheet_PRODUCT_MM_COMBINER_EP1_2017-06-20-14-42.pdf (accessed on 3 September 2018).
32. ITF Technologies, 3 × 1 Fiber Laser Combiner. Available online: http://www.itftechnologies.com/files/13/ITFT%20-%203x1%20FLC%20Rev.02_2018-01-26-16-56.pdf (accessed on 3 September 2018).
33. Martínez-Rios, A.; Torres-Gómez, I.; Monzon-Hernandez, D.; Barbosa-Garcia, O.; Duran-Ramirez, V.M. Reduction of Splice Loss between Dissimilar Fibers by Tapering and Fattening. *Rev. Mex. Física* **2010**, *56*. Available online: http://www.redalyc.org/articulo.oa?id=57016003012 (accessed on 3 September 2018).
34. Gattass, R.R.; Thapa, R.; Kung, F.H.; Busse, L.E.; Shaw, L.B.; Sanghera, J.S. Review of infrared fiber-based components. *Appl. Opt.* **2015**, *54*, F25–F34. [CrossRef] [PubMed]
35. Wu, J.; Sun, Y.; Wang, Y.; Li, T.; Feng, Y.; Ma, Y. The study of the thermally expanded core technique in end-pumped (N + 1) × 1 type combiner. *Proc. SPIE* **2015**, *9255*. [CrossRef]
36. Hanafusa, H.; Horiguchi, M.; Noda, J. Thermally-diffused expanded core fibres for low-loss and inexpensive photonic components. *Electron. Lett.* **1991**, *27*, 1968–1969. [CrossRef]
37. Kihara, M.; Matsumoto, M.; Haibara, T.; Tomita, S. Characteristics of thermally expanded core fiber. *J. Light. Technol.* **1996**, *14*, 2209–2214. [CrossRef]
38. Shiraishi, K.; Aizawa, Y.; Kawakami, S. Beam expanding fiber using thermal diffusion of the dopant. *J. Light. Technol.* **1990**, *8*, 1151–1161. [CrossRef]
39. Harper, J.S.; Botham, C.P.; Hornung, S. Tapers in single-mode optical fibre by controlled core diffusion. *Electron. Lett.* **1988**, *24*, 245–246. [CrossRef]
40. Wang, B.; Mies, E. Review of fabrication techniques for fused fiber components for fiber lasers. *Proc. SPIE* **2009**, *7195*. [CrossRef]
41. Snyder, A.W.; Love, J.D. *Optical Waveguide Theory*; Chapman and Hall: London, UK, 1983.
42. Marcuse, D. Loss analysis of single-mode fiber splices. *Bell Syst. Tech. J.* **1997**, *56*, 703. [CrossRef]
43. Fielding, A.J.; Edinger, K.; Davis, C.C. Experimental observation of mode evolution in single-mode tapered optical fibers. *J. Light. Technol.* **1999**, *17*, 1649. [CrossRef]
44. Love, J.D.; Henry, W.M. Quantifying loss minimisation in single-mode fibre tapers. *Electron. Lett.* **1986**, *22*, 912–914. [CrossRef]
45. Birks, T.A.; Li, Y.W. The shape of fiber tapers. *J. Light. Technol.* **1992**, *10*, 432–438. [CrossRef]
46. Saleh, B.E.A.; Teich, M.C. *Fundamentals of Photonics*, 2nd ed.; Wiley: Hoboken, NJ, USA, 1991.
47. Sévigny, B.; Poirier, P.; Faucher, M. Pump combiner loss as a function of input numerical aperture power distribution. *Proc. SPIE* **2009**, *7195*. [CrossRef]
48. Xiao, Q.; Ren, H.; Chen, X.; Yan, P.; Gong, M. Tapered Fiber Bundle 7 × 1 End-Pumping Coupler Capable of High Power CW Operation. *IEEE Photon. Technol. Lett.* **2013**, *25*, 2442–2445. [CrossRef]
49. Kim, J.K.; Hagemann, C.; Schreiber, T.; Peschel, T.; Böhme, S.; Eberhardt, R.; Tünnermann, A. Monolithic all-glass pump combiner scheme for high-power fiber laser systems. *Opt. Express* **2010**, *18*, 13194–13203. [CrossRef] [PubMed]
50. Wetter, A.; Faucher, M.; Lovelady, M.; Séguin, F. Tapered fused-bundle splitter capable of 1kW CW operation. *Proc. SPIE* **2007**, *6453*. [CrossRef]
51. Cao, Y.; Shi, W.; Sheng, Q.; Fu, S.; Zhang, H.; Bai, X.; Qi, L.; Yao, J. Investigation on high transmission efficiency 7 × 1 pump combiner. *Opt. Eng.* **2016**, *55*, 126102. [CrossRef]
52. Jauregui, C.; Böhme, S.; Wenetiadis, G.; Limpert, J.; Tünnermann, A. Side-pump combiner for all-fiber monolithic fiber lasers and amplifiers. *J. Opt. Soc. Am. B* **2010**, *27*, 1011–1015. [CrossRef]
53. Stachowiak, D.; Kaczmarek, P.; Abramski, K.M. High-power pump combiners for Tm-doped fibre lasers. *Opto-Electron. Rev.* **2015**, *23*, 259–264. [CrossRef]
54. Zhou, H.; Chen, Z.; Zhou, X.; Hou, J.; Chen, J. All-fiber 7 × 1 pump combiner for high power fiber laser. *Opt. Commun.* **2015**, *347*, 137–140. [CrossRef]
55. Xiao, Q.; Huang, Y.; Sun, J.; Wang, X.; Li, D.; Gong, M.; Yan, P. Research on multi-kilowatts level tapered fiber bundle N × 1 pumping combiner for high power fiber laser. *Front. Optoelectron.* **2016**, *9*, 301–305. [CrossRef]
56. Kim, B.H.; Kim, S.-J.; Yoon, Y.; Hann, S. Fabrication of the reliable (14 − 18) × 1 fiber laser power combiner by the novel double bundling method. *Proc. SPIE* **2013**, *8621*. [CrossRef]

57. Faucher, M.; Sevigny, B.; Perreault, R.; Wetter, A.; Holehouse, N. All-fiber 32 × 1 pump combiner with high isolation for high power fiber laser. In Proceedings of the 2008 Conference on Lasers and Electro-Optics and 2008 Conference on Quantum Electronics and Laser Science, San Jose, CA, USA, 4–9 May 2008; pp. 1–2. [CrossRef]
58. Neugroschl, D.; Park, J.; Wlodawski, M.; Singer, J.; Kopp, V.I. High-efficiency (6 + 1) × 1 combiner for high power fiber lasers and amplifiers. *Proc. SPIE* **2013**, *8601*. [CrossRef]
59. Theeg, T.; Sayinc, H.; Overmeyer, L.; Neumann, J.; Kracht, D. Manufacturing and optical characterization of side-pumped high power fiber combiner for LMA-fibers. In Proceedings of the 2015 European Conference on Lasers and Electro-Optics—European Quantum Electronics Conference, Munich, Germany, 21–25 June 2015; Optical Society of America: Washington, DC, USA Paper CE_2_4.
60. Koška, P.; Baravets, Y.; Peterka, P.; Bohata, J.; Písařík, M. Mode-field adapter for tapered-fiber-bundle signal and pump combiners. *Appl. Opt.* **2015**, *54*, 751–756. [CrossRef] [PubMed]
61. Koška, P.; Baravets, Y.; Peterka, P.; Písařík, M.; Bohata, J. Optimized mode-field adapter for low-loss fused fiber bundle signal and pump combiners. *Proc. SPIE* **2015**, *9344*. [CrossRef]
62. Theeg, T.; Sayinc, H.; Neumann, J.; Overmeyer, L.; Kracht, D. Pump and signal combiner for bi-directional pumping of all-fiber lasers and amplifiers. *Opt. Express* **2012**, *20*, 28125–28141. [CrossRef] [PubMed]
63. Sliwinska, D.; Kaczmarek, P.; Abramski, K.M. Tapered fiber bundle couplers for high-power fiber amplifiers. *Proc. SPIE* **2014**, *9441*. [CrossRef]
64. Theeg, T.; Sayinc, H.; Neumann, J.; Overmeyer, L.; Kracht, D. Side pumping scheme for all-fiber counter-pumping of high power single-frequency fiber amplifiers. In Proceedings of the 2013 Conference on Lasers & Electro-Optics Europe & International Quantum Electronics Conference CLEO EUROPE/IQEC, Munich, Germany, 12–16 May 2013. [CrossRef]
65. Stachowiak, D.; Kaczmarek, P.; Abramski, K.M. (5 + 1) × 1 pump and signal power combiner with 9/80 µm feed-through signal fiber. *Opt. Laser Technol.* **2017**, *93*, 33–40. [CrossRef]
66. Zhao, K.; Chang, X.; Chen, Z.; Wang, Z.; Jiang, H. Fabrication of high-efficiency pump and signal combiner based on a thermally expanded core technique. *Opt. Laser Technol.* **2015**, *75*, 1–5. [CrossRef]
67. Kopp, V.I.; Park, J.; Wlodawski, M.; Singer, J.; Neugroschl, D. Polarization maintaining, high-power and high-efficiency (6 + 1) × 1 pump/signal combiner. *Proc. SPIE* **2014**, *8961*. [CrossRef]
68. Zou, S.; Chen, H.; Yu, H.; Sun, J.; Zhao, P.; Lin, X. High-efficiency (6 + 1) × 1 pump-signal combiner based on low-deformation and high-precision alignment fabrication. *Appl. Phys. B* **2017**, *123*, 288. [CrossRef]
69. Zheng, J.; Zhao, W.; Zhao, B.; Li, Z.; Chang, C.; Li, G.; Gao, Q.; Ju, P.; Gao, W.; She, S.; et al. High pumping- power fiber combiner for double-cladding fiber lasers and amplifiers. *Opt. Eng.* **2018**, *57*, 036105. [CrossRef]
70. Liu, K.; Zhao, C.; Yang, Y.; Chen, X.; Wang, J.; He, B.; Zhou, J. Low beam quality degradation, high-efficiency pump and signal combiner by built-in mode field adapter. *Appl. Opt.* **2017**, *56*, 2804–2809. [CrossRef] [PubMed]
71. Noordegraaf, D.; Maack, M.D.; Skovgaard, P.M.W.; Agger, S.; Alkeskjold, T.T.; Lægsgaard, J. 7 + 1 to 1 pump/signal combiner for air-clad fiber with 15 µm MFD PM single-mode signal feed-through. *Proc. SPIE* **2010**, *7580*. [CrossRef]
72. Xiao, Q.; Yan, P.; Ren, H.; Chen, X.; Gong, M. Pump-signal combiner with large-core signal fiber feed-through for fiber lasers and amplifiers. *Appl. Opt.* **2013**, *52*, 409–414. [CrossRef] [PubMed]
73. Braglia, A.; Califano, A.; Olivero, M.; Penna, A.; Perrone, G. All-fiber kilowatt signal combiners for high power fiber lasers. In Proceedings of the 2013 Conference on Lasers & Electro-Optics Europe & International Quantum Electronics Conference CLEO EUROPE/IQEC, Munich, Germany, 12–16 May 2013. [CrossRef]
74. Wickham, M.; Cheung, E.C.; Ho, J.G.; Goodno, G.D.; Rice, R.R.; Rothenberg, J.; Thielen, P.; Weber, M. Coherent Combination of Fiber Lasers with a Diffractive Optical Element. *OSA Proc. Adv. Solid-State Photonics* **2008**, WA5. [CrossRef]
75. Shamir, Y.; Sintov, Y.; Shtaif, M. Incoherent beam combining of multiple single-mode fiber lasers utilizing fused tapered bundling. *Proc. SPIE* **2010**, *7580*. [CrossRef]
76. Zhou, H.; Chen, Z.; Zhou, X.; Hou, J.; Chen, J. All-fiber 7 × 1 signal combiner with high beam quality for high-power fiber lasers. *Chin. Opt. Lett.* **2015**, *13*, 061406. [CrossRef]
77. Loftus, T.H.; Liu, A.; Hoffman, P.R.; Thomas, A.M.; Norsen, M.; Royse, R.; Honea, E. 522 W average power, spectrally beam-combined fiber laser with near-diffraction-limited beam quality. *Opt. Lett.* **2007**, *32*, 349–351. [CrossRef] [PubMed]

78. Shamir, Y.; Sintov, Y.; Shtaif, M. Large-mode-area fused-fiber combiners, with nearly lowest-mode brightness conservation. *Opt. Lett.* **2011**, *36*, 2874–2876. [CrossRef] [PubMed]
79. Shamir, Y.; Zuitlin, R.; Sintov, Y.; Shtaif, M. 3kW-level incoherent and coherent mode combining via all-fiber fused Y-couplers. In *Frontiers in Optics 2012/Laser Science XXVIII*; Optical Society of America: Washington, DC, USA, 2012.
80. Noordegraaf, D.; Maack, M.D.; Skovgaard, P.M.W.; Johansen, J.; Becker, F.; Belke, S.; Blomqvist, M.; Laegsgaard, J. All-fiber 7 × 1 signal combiner for incoherent laser beam combining. *Proc. SPIE* **2011**, *7914*. [CrossRef]
81. Zhou, H.; Jin, A.; Chen, Z.; Zhang, B.; Zhou, X.; Chen, S.; Hou, J.; Chen, J. Combined supercontinuum source with >200 W power using a 3 × 1 broadband fiber power combiner. *Opt. Lett.* **2015**, *40*, 3810–3813. [CrossRef] [PubMed]
82. Zhou, X.; Chen, Z.; Wang, Z.; Hou, J.; Xu, X. Beam Quality Analysis of Incoherent Beam Combining by a 7 × 1 All-Fiber Signal Combiner. *IEEE Photon. Technol. Lett.* **2016**, *28*, 2265–2268. [CrossRef]
83. Lei, C.; Gu, Y.; Chen, Z.; Wang, Z.; Zhou, P.; Ma, Y.; Xiao, H.; Leng, J.; Wang, X.; Hou, J.; et al. Incoherent beam combining of fiber lasers by an all-fiber 7 × 1 signal combiner at a power level of 14 kW. *Opt. Express* **2018**, *26*, 10421–10427. [CrossRef] [PubMed]
84. Zhou, H.; Chen, Z.; Zhou, X.; Hou, J.; Chen, J. All-fiber 7 × 1 signal combiner for high power fiber lasers. *Appl. Opt.* **2015**, *54*, 3090–3094. [CrossRef] [PubMed]
85. Malka, D.; Cohen, E.; Zalevsky, Z. Design of 4 × 1 Power Beam Combiner Based on MultiCore Photonic Crystal Fiber. *Appl. Sci.* **2017**, *7*, 695. [CrossRef]
86. Nielsen, M.D.; Srensen, M.H.; Liem, A.; Kozak, M.; Skovgaard, P.M. High power PCF-based pump combiners. *Proc. SPIE* **2007**, *6453*. [CrossRef]
87. Hansen, K.P.; Olausson, C.B.; Broeng, J.; Noordegraaf, D.; Maack, M.D.; Alkeskjold, T.T.; Laurila, M.; Nikolajsen, T.; Skovgaard, P.M.W.; Srensen, M.H.; et al. Airclad fiber laser technology. *Opt. Eng.* **2011**, *50*, 111609. [CrossRef]
88. Ishikura, A.; Kato, Y.; Miyauchi, M. Taper splice method for single-mode fibers. *Appl. Opt.* **1986**, *25*, 3460–3465. [CrossRef] [PubMed]
89. Kihara, M.; Tomita, S.; Matsumoto, M. Loss characteristics of thermally diffused expanded core fiber. *IEEE Photon. Technol. Lett.* **1992**, *4*, 1390–1391. [CrossRef]
90. Shigihara, K.; Shiraishi, K.; Kawakami, S. Modal field transforming fiber between dissimilar waveguides. *J. Appl. Phys.* **1986**, *60*, 4293–4296. [CrossRef]
91. Faucher, M.; Lize, Y.K. Mode field adaptation for high power fiber lasers. In Proceedings of the Conference Lasers and Electro-Optics, San Jose, CA, USA, 6–11 May 2007. [CrossRef]
92. Mafi, A.; Hofmann, P.; Jollivet Salvin, C.; Schülzgen, A. Low-loss coupling between two single-mode optical fibers with different mode-field diameters using a graded-index multimode optical fiber. *Opt. Lett.* **2011**, *36*, 3596–3598. [CrossRef] [PubMed]
93. Hofmann, P.; Mafi, A.; Jollivet, C.; Tiess, T.; Peyghambarian, N.; Schulzgen, A. Detailed Investigation of Mode-Field Adapters Utilizing Multimode-Interference in Graded Index Fibers. *J. Light. Technol.* **2012**, *30*, 2289–2298. [CrossRef]
94. Zhou, X.; Chen, Z.; Chen, H.; Li, J.; Hou, J. Mode field adaptation between single-mode fiber and large mode area fiber by thermally expanded core technique. *Opt. Laser Technol.* **2013**, *47*, 72–75. [CrossRef]
95. Zhou, X.; Chen, Z.; Zhou, H.; Hou, J. Mode-field adaptor between large-mode-area fiber and single-mode fiber based on fiber tapering and thermally expanded core technique. *Appl. Opt.* **2014**, *53*, 5053–5057. [CrossRef] [PubMed]
96. Kaczmarek, P.; Stachowiak, D.; Abramski, K.M. 40 W All-Fiber Er/Yb MOPA System Using Self-Fabricated High-Power Passive Fiber Components. *Appl. Sci.* **2018**, *8*, 869. [CrossRef]